An electromagnetic analogy of quantum wells: guided plasmon resonances coupled to transverse electromagnetic waves in multilayered systems

RAÚL ALFONSO VÁZQUEZ-NAVA

Facultad de Ciencias, Universidad Autónoma del Estado de Morelos
Colonia Chamilpa, 62000 Cuernavaca, Mor., Mexico

MARCELO DEL CASTILLO-MUSSOT, GERARDO J. VÁZQUEZ, AND CARLOS I. MENDOZA

Instituto de Física, Universidad Nacional Autónoma de México
Apartado postal 20-364, 01000 México D.F., Mexico

ABSTRACT. We present calculations for the electromagnetic reflectance spectra of finite multilayered systems (superlattices) made of very thin films of different thickness. In contrast to quantum resonances, for which there is only one kind of propagating waves, the electromagnetic resonances exhibited by these systems for non normal incidence are due to the longitudinal electromagnetic waves (or guided plasmons) coupled to the usual long-wavelength transverse electromagnetic waves. We employ a transfer matrix formalism for the layered system together with a hydrodynamic model for the electron dynamics. For realistic values of film thickness, a larger number of such resonances could be observed in multilayered systems formed by highly doped semiconductor layers rather than in systems formed by metallic layers.

RESUMEN. Presentamos cálculos de espectros de reflectancia electromagnética de sistemas finitos de multicapas (superredes), hechas de películas muy delgadas de diferentes anchos. A diferencia de las resonancias cuánticas, para las cuales hay un sólo tipo de ondas que se propagan, las resonancias electromagnéticas mostradas por estos sistemas en incidencia no normal son debidas a las ondas electromagnéticas longitudinales (plasmones guiados) acopladas a las bien conocidas ondas electromagnéticas transversales. Utilizamos el formalismo de la matriz de transferencia para el sistema de multicapas junto con el modelo hidrodinámico para la dinámica de los electrones. Para valores realistas de los anchos de las películas de estos sistemas de multicapas, se pueden observar un mayor número de resonancias en sistemas formados por capas de semiconductores altamente dopados que en sistemas formados por capas metálicas.

1. INTRODUCTION

1.1. ANALOGIES BETWEEN QUANTUM AND ELECTROMAGNETIC WAVES

Within the spirit of establishing useful analogies in the propagation of waves between quantum mechanics and other fields of physics, the one-particle propagation in one-

dimensional multiple quantum well systems has been compared with the propagation of transverse electromagnetic waves in stratified media. An appropriate mathematical tool to describe quantum mechanical, electromagnetic and elastic phenomena in layered media is the transfer matrix formalism [1].

As we will see, they can propagate in material media two kinds of electromagnetic waves; the well known transverse waves (for example, infrared and optical among others) and the longitudinal waves. In a homogeneous media the former have the electric field $\mathbf{E}$ perpendicular to the direction of propagation $\mathbf{q}$, whereas the latter have $\mathbf{E}$ and $\mathbf{q}$ parallel.

In this article we apply the transfer matrix formalism to systems made of layers of different thicknesses, where both longitudinal (L) and transverse (T) electromagnetic waves are present together with the so called hydrodynamic model which describes the dynamics of the charged carriers. We also discuss the L-T coupling in interfaces, the propagation of confined L waves (or guided plasmons) and their effects in the reflectance of multilayered systems.

1.2. LONGITUDINAL AND TRANSVERSE ELECTROMAGNETIC WAVES AS SOLUTIONS OF MAXWELL EQUATIONS

To show how both longitudinal and transverse electromagnetic waves arise from first principles we take

$$\mathbf{E}\left(\mathbf{r}, t\right) = \mathbf{E} \exp\left[i(\mathbf{q} \cdot \mathbf{r} - \omega t)\right] \tag{1}$$

and

$$\mathbf{B}\left(\mathbf{r}, t\right) = \mathbf{B} \exp\left[i(\mathbf{q} \cdot \mathbf{r} - \omega t)\right] \tag{2}$$

together with Maxwell's equations to get

$$\left[q^2 \delta_{ij} - q_i q_j - \left(\omega^2/c^2\right) \varepsilon_{ij}\left(\mathbf{q}, \omega\right)\right] E_j = 0, \qquad i = 1, 2, 3, \tag{3}$$

where ε_{ij} are the components of the dielectric tensor. In general it is convenient to write the solutions of the last equation in the form $\mathbf{q} = \mathbf{q}\left(\omega\right)$, with ω real and $\mathbf{q}$ complex, or $\omega = \omega\left(\mathbf{q}\right)$, with $\mathbf{q}$ real and ω complex; these are the dispersion relations for the electromagnetic waves. If the medium is isotropic $\varepsilon_{ij}\left(\mathbf{q}, \omega\right)$ can be written in the form

$$\varepsilon_{ij}\left(\mathbf{q}, \omega\right) = P_{ij}^{\mathrm{L}} \varepsilon_{\mathrm{L}}\left(q, \omega\right) + P_{ij}^{\mathrm{T}} \varepsilon_{\mathrm{T}}\left(q, \omega\right), \tag{4}$$

where we have introduced longitudinal and transverse projection (tensors)

$$P_{ij}^{\mathrm{L}} = q_i q_j / q^2, \qquad P_{ij}^{\mathrm{T}} = \delta_{ij} - P_{ij}^{\mathrm{L}} \tag{5}$$

and the longitudinal and transverse dielectric functions $\varepsilon_{\mathrm{L}}(q, \omega)$ and $\varepsilon_{\mathrm{T}}(q, \omega)$, which are scalars. By writing $\mathbf{E}$ as a sum of transverse and longitudinal components,

$$\mathbf{E} = \left(\mathbf{P}^{\mathrm{L}} + \mathbf{P}^{\mathrm{T}}\right) \mathbf{E} = \mathbf{E}_{\mathrm{L}} + \mathbf{E}_{\mathrm{T}}, \tag{6}$$

we can decompose Eq. (3) into separate equations for the transverse and longitudinal fields:

$$\left[q^2 - \left(\omega^2/c^2 \right) \varepsilon_{\mathrm{T}}\left(q, \omega \right) \right] E_{\mathrm{T}} = 0, \tag{7}$$

$$\varepsilon_{\mathrm{L}}\left(q, \omega \right) \mathbf{E}_{\mathrm{L}} = 0. \tag{8}$$

Therefore, the dispersion relation for transverse waves for which $\mathbf{q} \cdot \mathbf{E} = 0$, is the solution of

$$\left[q^2 - \left(\omega^2/c^2 \right) \varepsilon_{\mathrm{T}}\left(q, \omega \right) \right] = 0, \tag{9}$$

and the dispersion relation for longitudinal waves, for which $\mathbf{q} \times \mathbf{E} = 0$ and $\mathbf{B} = 0$, is the solution of

$$\varepsilon_{\mathrm{L}}\left(q, \omega \right) = 0. \tag{10}$$

This decomposition of $\mathbf{E}$ and ε_{ij} into transverse and longitudinal components is valid if the wave vector is complex, $\mathbf{q} = \mathbf{q}' + i\mathbf{q}''$, with the real and imaginary parts in different directions. In this case, the conditions $\mathbf{q} \cdot \mathbf{E} = 0$ or $\mathbf{q} \times \mathbf{E} = 0$ do not signify that $\mathbf{q}$ is perpendicular or parallel to $\mathbf{E}$, since $\mathbf{q}$ does not have a definite direction.

1.3. Hydrodynamic model

To go beyond local models for the dielectric function of an electron gas (such as the common Drude model) we can use the hydrodynamic model or hydrodynamic approximation to take into account in a simple manner that the carriers form a compressible gas. In this approximation the dielectric function is calculated by neglecting the thermal velocity of the particles; only the average velocity $\mathbf{u}$ appears. Let us consider an electron gas with no static applied electric and magnetic fields ($\mathbf{E}_0 = 0$ and $\mathbf{B}_0 = 0$) and use a linearization procedure in small induced quantities such as $\mathbf{E}$, $\mathbf{B}$, fluctuation current density $\mathbf{j}$, etc. That is in the following derivation of the dielectric tensor we will make use of a linearization procedure in which fields such as $\mathbf{E}$ and $\mathbf{B}$ and the average particle velocity (often referred to as drift velocity) associated with the electromagnetic waves are considered to be small quantities. For simplicity we model the ions as a homogeneous positive background (jellium model) in order to keep the system electrically neutral. The equation of motion of the electrons is [2]

$$m \frac{d\mathbf{u}}{dt} = -e \left[\mathbf{E} + \left(\frac{\mathbf{u}}{c} \right) \times \mathbf{B} \right] - \frac{\nabla p}{\rho}, \tag{11}$$

where m and e are the mass and charge of the electrons and ρ is the charge-density fluctuation induced in the electron gas. The last term in Eq. (11) would not be included in the local Drude model. Some many-body effects are taken into account partially by the last term which represents the force per particle due to the pressure gradient ∇p. The negative sign of this term indicates, as expected, that particles tend to move away from high density regions. We could also have included a term proportional to the velocity simulating the damping force due to collisions. Since $\nabla p = (\delta p / \delta \rho) \nabla \rho$, we can define

a characteristic velocity β by $\beta^2 = (\delta p/\delta \rho)$ and use the equation of state $p = p(\rho)$ to relate this velocity to the thermal velocity in a classical gas and to the Fermi velocity in a degenerate gas. β is called the "stiffness" of the gas, since it measures its compressibility and is responsible for the spatial dispersion or nonlocality. One can use the equation of continuity (or conservation of particle number)

$$\frac{\delta \rho}{\delta t} + \nabla \cdot (\rho \mathbf{u}) = 0, \tag{12}$$

to linearize Eq. (11) to get

$$-i\omega \mathbf{u} = -\frac{e\mathbf{E}}{m} - \frac{\beta^2 i \mathbf{q}(\mathbf{q} \cdot \mathbf{u})}{\omega}, \tag{13}$$

where we have neglected the term containing $(\mathbf{u}/c) \times \mathbf{B}$. For definiteness, it is convenient to take $\mathbf{q}$ in the z direction. Then $\varepsilon_{zz} \equiv \varepsilon_{\mathrm{L}}(q,\omega)$, the longitudinal dielectric function, $\varepsilon_{xx} = \varepsilon_{yy} \equiv \varepsilon_{\mathrm{T}}(q,\omega)$, the transverse dielectric function, and $\varepsilon_{ij} = 0$ if $i \neq j$. From $\mathbf{j} = -e\rho \mathbf{u}$ and

$$\mathrm{j}_i(\mathbf{q},\omega) = \sigma_{ij}(\mathbf{q},\omega)\,\mathrm{E}_j(\mathbf{q},\omega), \tag{14}$$

$$\varepsilon_{ij}(\mathbf{q},\omega) = \delta_{ij} + (4\pi i/\omega)\,\sigma_{ij}(\mathbf{q},\omega), \tag{15}$$

we find

$$\varepsilon_{\mathrm{L}}(q,\omega) = 1 - \frac{\omega_p^2}{(\omega - \beta^2 q^2)}, \tag{16}$$

$$\varepsilon_{\mathrm{T}}(\omega) = 1 - \frac{\omega_p^2}{\omega^2}, \tag{17}$$

where $\omega_p = (4\pi \rho e^2/m)$ is the plasma frequency of the electron gas. The absence of q-dependence of Drude-like ε_{T} indicates that the pressure gradient force does not affect the components of ε that describe transverse motion, where there is no density change. For a degenerate electron gas we choose $\beta^2 = 3v_F^2/5$, where v_F is the Fermi velocity. This value can be obtained from a long-wavelength expansion of Lindhard's dielectric response model [3], which is a better model for the dynamics of the electron gas than the hydrodynamic model. The hydrodynamic model can also include the contribution of bounded electrons and the effect of collisions to yield

$$\varepsilon_{\mathrm{L}}(q,\omega) = \varepsilon_{\mathrm{B}}(\omega) - \frac{\omega_p^2}{(\omega + i\omega/\tau - \beta^2 q^2)}, \tag{18}$$

$$\varepsilon_{\mathrm{T}}(q,\omega) = \varepsilon_{\mathrm{B}}(\omega) - \frac{\omega_p^2}{(\omega + i\omega/\tau)}, \tag{19}$$

where ε_{B} is the bound electron contribution to the dielectric response (which in general depends on the frequency ω) and τ is a phenomenological damping constant which arises from a trivial generalization of Eq. (10) if a friction force is included. The dependence of the dielectric function on $\mathbf{q}$ makes the hydrodynamic model a nonlocal one.
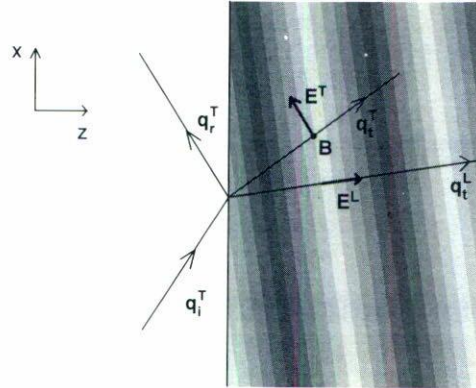
FIGURE 1. Vacuum-conductor interface. Within a non local model the wave vectors of the transverse (T) and longitudinal (L) waves are shown together with associated electric and magnetic in the conductor. Incident, reflected and transmitted waves are indicated by the subscripts i, r and t, respectively. The charge density fluctuations produced by the longitudinal wave are schematically depicted by the different shaded regions.

A detailed analysis of the dispersion relations [Eqs. (9) and (10)] shows that in the hydrodynamic approximation the ratio of the wavelengths $\lambda_T/\lambda_L \simeq c/\beta \simeq c/v_F$ is large, which means that λ_L is small. Thus, the resonances due to longitudinal waves ("longitudinal" Fabry-Perot resonances) are better observed in thin films [4]. Experimental and theoretical work on the effects of spatial dispersion or nonlocality are found in Refs. 4 and 5, respectively. Nonlocality can be taken into account by including longitudinal plasmons (as in our work) or electron-hole pairs creation.

2. APPLICATIONS TO MULTILAYERED SYSTEMS

2.1. COUPLING OF LONGITUDINAL AND ELECTROMAGNETIC WAVES AT AN INTERFACE

It was shown in Sect. 1.2 that in a homogeneous medium transverse (T) waves are not coupled to longitudinal (L) waves. In other words, in a homogeneous medium longitudinal waves cannot be excited by light or other electromagnetic waves consisting of transverse waves. However, the presence of an interface can produce L-T coupling [4, 5] due to the following process. Let us consider, for simplicity, the simple case of an transverse p-polarized wave (for which the electric field lies on the plane of incidence) traveling from vacuum to a non-local medium. For non normal incidence, the normal component of the total electric field in the non-local medium does not vanish, and the impinging wave will generate reflected and transmitted transverse waves, and one longitudinal wave as shown. This longitudinal wave is produced by $\mathbf{E}_z$ which compresses the carriers towards the barrier at the interface. In other words, the physical mechanism that allows the generation of plasmons by transverse waves consists of the confinement of the moving charges by the interface, which in turn produces regions of lower and higher compressibility. In Fig. 1 we depict the resulting waves produced by an incident transverse wave on a vacuum-insulator interface. In contrast to transverse waves , which propagate either in
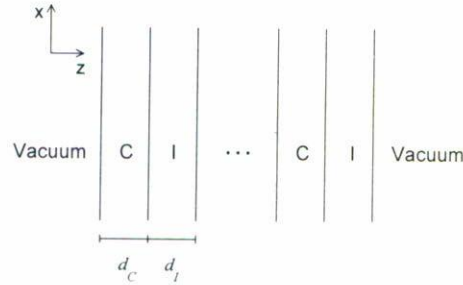
FIGURE 2. Finite system of alternating conducting (C) and insulating (I) layers in vacuum.

vacuum or material media, the longitudinal waves only propagate in material media and they are better observed in very thin layers of thickness d for which $\lambda_{\mathrm{L}} \simeq d$. It must be emphasized that these plasmons are excitations that occur in the *bulk* and thus should not be confused with the electromagnetic surface plasmons.

Here we present an example of resonances formed by plasmons or longitudinal electromagnetic waves in a electron gas coupled to transverse electromagnetic waves in the interfaces of multilayered systems (or superlattices) consisting of alternating insulating and conducting layers, as shown in Fig. 2. Therefore, in each conductor, such resonances can be regarded as guided plasma waves interacting among themselves. The conducting layers of the superlattice must have free carriers, so they can be made either of metals or highly doped semiconductors. For the latter case our formalism would describe the electrons in the conduction band of the semiconductor.

2.2. TRANSFER MATRIX FORMALISM

Let us consider a multilayered system consisting of alternating insulating and conducting layers, stacked along the z direction, on which p-polarized (that is, plane-polarized transverse waves where the electric field lies on the plane of incidence xz) and longitudinal waves (or plasmons) propagate (see Fig. 2). In an isotropic system there is no coupling of transverse and longitudinal waves. However, as mentioned before the presence of the interface and p-polarized waves allows such coupling. We do not consider s-polarized waves since they do not couple to longitudinal plasmons. In what follows me may use indistinctly the terms electromagnetic longitudinal wave or plasmon.

It is convenient to make use of the simple transfer-matrix formalism developed in Ref. 6 to study the effect of plasma waves on the electromagnetic modes and the reflectance of conductor-insulator superlattices. This formalism takes into account, within the hydrodynamic model, the nonlocal effects (or spatial dispersion) due to the presence of plasmons and their coupling to transverse waves. Thus, the construction of the transfer matrix involves two p-polarized waves; one with positive and other with negative component of the wave vector along the z direction, that is, $\mathbf{K} = (Q, 0, \pm k)$ obeying

$$k^2 = \frac{\varepsilon_C(\omega)\,\omega^2}{c^2} - Q^2, \tag{20}$$

and two longitudinal waves with wave vector $\mathbf{l}_\pm = (Q, 0, \pm l)$ obeying

$$\varepsilon_C^l (\mathbf{l}_\pm, \omega) = 0, \tag{21}$$

where ε_C is the transverse and ε_C^l the longitudinal dielectric function of the conductor. For sharp interfaces it is shown [5] how the conductor's 4×4 transfer matrix collapses to a 2×2 matrix whenever the film is bounded in both sides by insulators, as in our case. As usual, the reflectance $R = |r|^2$ of an n-layer superlattice is given, in terms of the impedances of the vacuum Z_v and of the superlattice and Z by

$$r = \frac{Z_v - Z}{Z_v + Z}, \tag{22}$$

and

$$Z = \frac{Z_v M_{22} - M_{12}}{M_{11} - Z_v M_{21}}, \tag{23}$$

where $\mathbf{M}$ is the 2×2 transfer matrix of the full superlattice resulting from the product of all n transfer matrices. For instance, the transfer matrix $\mathbf{M} = \mathbf{M}_I \mathbf{M}_C$ corresponding to a system of one conductor and one insulator is given by Eq. (24) of Ref. 6.

As in the electronic band structure of solids where there is a periodic arrangement of atoms, a periodic arrangement of layers can produce allowed and forbidden bands in the propagation of electromagnetic waves. In Ref. 6 the presence of such bands in the propagation of coupled transverse and longitudinal electromagnetic bands was shown. The transfer-matrix formalism summarized above was employed in Ref. 6 to calculate the properties of periodic (and infinite) superlattices and in this article this formalism will be applied to finite superlattices.

2.3. NUMERICAL RESULTS

Figure 3 shows our calculation for the reflectance of a very thin ($d = 30$ Å) single metal film where the free-electron data for aluminum [7,8] ($\varepsilon_B = 1$) were used. There are propagating bulk modes, made up of "guided" plasmons, in frequencies where no propagation is expected if spatial dispersion or longitudinal plasmons are neglected. Within the hydrodynamic model these modes manifest themselves as a series of sharp peaks in the reflectance spectra due to the strong mismatch of impedances near the single- film resonance frequencies ω_n given, as indicated by Eq. (10), by approximately the zeros of

$$\varepsilon_C^l (\mathbf{l}_\pm, \omega) = \varepsilon_B - \frac{\omega_p^2}{[\omega + i\omega/\tau - \beta^2 (Q^2 + l^2)]}, \tag{24}$$

where l, the z-component of the wavevector is quantized and equal to $n\pi/d$ (or $d = n\lambda/2$). These frequencies are given by

$$\omega_n^2 = \frac{\omega_p^2}{\varepsilon_B} + \beta^2 \left[Q^2 + \left(\frac{n\pi}{d} \right)^2 \right], \qquad n = 1, 2, 3, \dots . \tag{25}$$
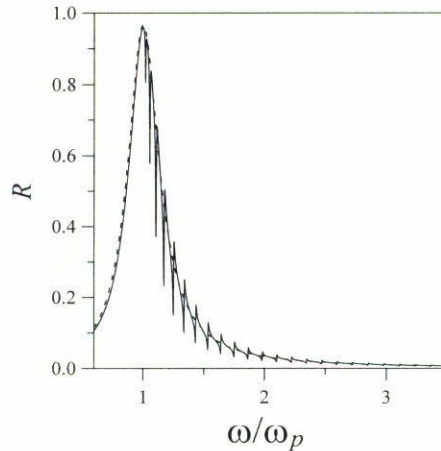
FIGURE 3. Local (dashed line)and nonlocal (solid line) calculation of the electromagnetic reflectance of a *metallic* film of width $d_M = 30$ Å for an angle of incidence $\theta = 70°$ described by Drude transverse dielectric function and hydrodynamic longitudinal dielectric function both with $\varepsilon_B = 1$. We chose for the film the values corresponding to the free-electron data for aluminium [7,8]; $N_0 = 1.81 \times 10^{23}$ cm^{-3}, $\hbar\omega_p = 14.7$ eV, $\tau = 192/\omega_p$ and $\beta = 5.23 \times 10^{-3}c$, where c is the speed of light. For simplicity we chose for the insulator $\varepsilon_I = 1$.

These guided plasmons are coupled among themselves by only the long-wavelength transverse waves they induce in the insulating layers since there are no longitudinal waves in the insulator layers. The sharp structure of the non local calculation corresponds to the frequencies of the odd-numbered guided plasma waves [odd n in Eq. (25)], whereas the even numbered plasmons are barely noticeable, since when n is even the electric field outside the conducting films is very small (in this case each film is similar to a capacitor, except from a smooth charge modulation along the x direction given by e^{iQx}). The detailed shape of the features in the reflectance spectra depends obviously of the strength of the coupling between transverse and longitudinal waves at the interface. This coupling, in turn, is sensitive to the microscopic surface structure. For example, in more complete models such as the RPA self-consistent jellium, in which the electronic density does not fall sharply to zero at the interface and in which excitation of electron hole pairs is possible, this coupling is smaller than in the hydrodynamic model [9]. However, the presence of the main features of the resonant structure within the hydrodynamic model seems to remain in any better non-local theory.

If we compare these results with those of an infinite superlattice [6], we notice that the main differences are the following. In the first place, the local calculations in the infinite and finite case (without longitudinal plasmons) have a very different shape, and as we will see in the next figures, the shape remains practically the same in the finite case when the number of layers is small. This is due to the fact that the wavelength of the transverse wave (which is reponsible for the local result) is much larger than the width of the superlattice (recall that $\lambda_T/\lambda_L \simeq c/\beta$). In second place, as expected from Eq. (25), the resonances due to the guided plasmons are more localized in frequency in the periodic case (since all conducting layers have the same width) than in the finite case for which we chose different widths.
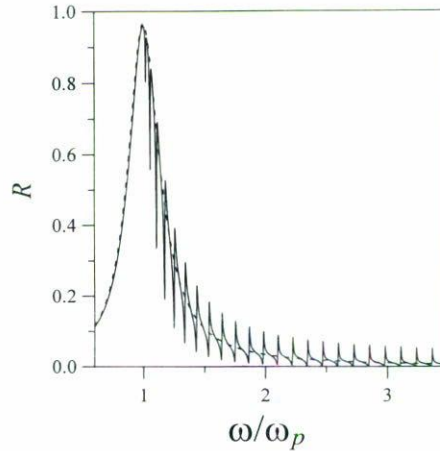
FIGURE 4. Same as Fig. 2, but with $\varepsilon_B(\omega)$ adjusted to the optical experimental data of aluminum as it was done in Ref. 9 to incorporate the bound electron contribution.

In Fig. 4 we follow a modified hydrodynamic model [10] for aluminum to include the contribution from bound electrons, in which $\varepsilon_B(\omega)$ is adjusted to fit the experimental local dielectric function $\varepsilon_{\exp}(\omega)$ from the measured refractive index data [7] according to

$$\varepsilon_B(\omega) = \varepsilon_{\exp}(\omega) + \frac{\omega_p}{(\omega + i\omega/\tau)}. \tag{26}$$

The structure obtained in the reflectance is similar to that of Fig. 3, but with the guided plasmon peaks slightly sharper that in the simpler model corresponding to $\varepsilon_B(\omega) = 1$. Also, from Eq. (25), it can be seen that for a single film plasmon resonances get closer in frequency when the thickness of the film is increased. We note that in both figures the resonances lie very close together, so it will be difficult, within the experimental range of thin films, to accommodate more resonances in multilayer systems within a given range in units of ω/ω_p. To look for the same resonances in similar systems, we calculated in Fig. 5 the reflectance spectra of *four* highly-doped semiconductor films where the width of the semiconductor films decreases linearly (alternated with vacuum layers), for which the same Drude and hydrodynamic models apply, but due to much smaller electronic density than in a metal (approximately 10^6 times smaller), the same number of guided plasmon resonances lie over a wider range of frequencies (in units of the plasma frequency) than in the metal films of the same width. This is due to the fact that for a single layer of constant width the separation between peaks is proportional to $\beta^2/\omega_p \propto N_0^{2/3}/N_0 = N_0^{-1/3}$, being N_0 the conduction electronic density. We also introduced for a doped semiconductor a larger τ than in a metal, since for both metals and semiconductors, τ could be expressed as the time between two successive collisions $\tau = s/v$, (s is the distance between two succesive collisions and v is the random velocity which, in turn, is of the order of the Fermi velocity), being s approximately the same for metals and semiconductors and v much larger for semiconductors. On the other hand, since the region around the minimum of the conduction band in typical semiconductors does not overlap with other bands, the Drude model can be applied for the electrons
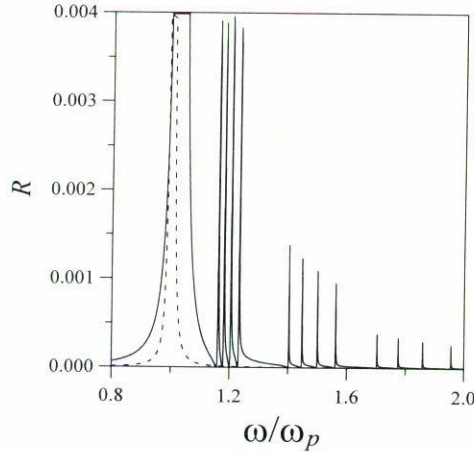
FIGURE 5. Nonlocal calculation of the electromagnetic reflectance for an angle of incidence $\theta = 70°$ of a superlattice made of alternating vacuum layers ($\varepsilon_I = 1$) and four highly-doped semiconductor layers. The layer that lies closer to the incident radiation has the width $d_S^{(1)}$ and the width of all the insulating layers are the same; $d_I = 100$ Å. The widths are consecutively decreased 6 Å, that is; $d_S^{(1)} = 100$ Å, $d_S^{(2)} = 94$ Å, $d_S^{(3)} = 88$ Å and $d = 82$ Å. Each film is described by Drude transverse dielectric function and hydrodynamic longitudinal dielectric function both with $\varepsilon_B = 1$. The parameters we chose for the film are $\tau = 1000/\omega_p$, $N_0 = 2.33 \times 10^{17}$ cm^{-3}, $\hbar\omega_p = 1.67 \times 10^{-2}$ eV, and $\beta = 5.70 \times 10^{-5}c$, where c is the speed of light. In the definition of the plasma frequency we use for simplicity the bare mass of the electron as the effective mass.

populating the conduction band of a semiconductor. In other words, in general it is not necessary to improve the Drude model by including the bound electron contribution ($\varepsilon_B(\omega) \neq 1$) as we did in Fig. 5, in metals.

In Fig. 6 we calculated the reflectance spectra of a system made of *six* higly-doped semiconductor layers with alternating insulator layers, where again the width of the semiconductor films was also choose to decrease linearly. Figure 7 is the same as Fig. 6, but with a a logarithmic scale in the vertical axis in order to appreciate the relative heights of all the peaks in the reflectance. Since the wavelength of the transverse waves is much larger than the wavelength of the longitudinal waves, we always chose for the insulator films a constant width and $\varepsilon_I = 1$. That is, the reflectance of the system is not sensitive to the composition or width of the insulating layers. In all calculations shown here, the intensity of the guided plasmon peaks is almost the same in both a single-film system and in a multilayered system. This comparison shows how weak the interactions are among such guided plasmons.

Concerning the separation of the guided plasmons peaks in Figs. 5, 6, and 7 we notice that we obtained for each family associated to a n-resonance an n-dependent separation $\Delta\omega_n$. The latter figures shows a region of frequencies where peaks of the families corresponding to $n = 5$ and 7 mix. The separation of the resonances $\Delta\omega_n$ is not constant since a constant separation would require, instead of a simple linear dependence of the width of the films, a more complicated dependence to adjust the widths. In the case of a large number of layers of the same or similar width each family (labeled by n) will produce a n-band of longitudinal plasmons.
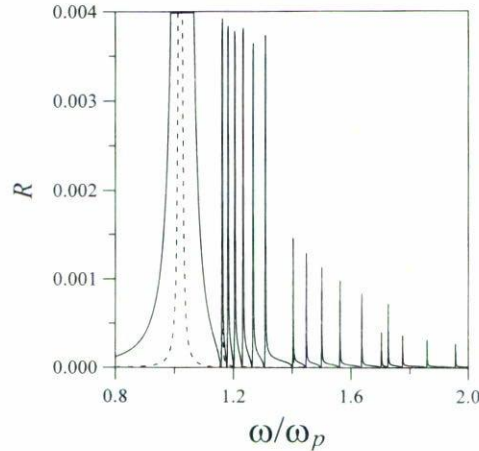
FIGURE 6. Same as Fig. 4, but instead of four layers there are six semiconductor layers with widths decreased also 6 Å, that is, $d_S^{(1)} = 100$ Å, ..., $d_S^{(6)} = 70$ Å.
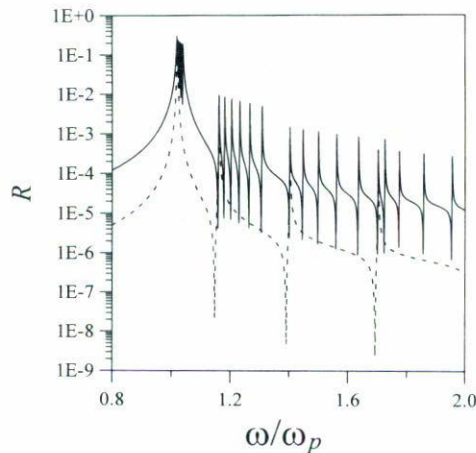

FIGURE 7. Same as Fig. 5, but with a a logarithmic scale in the vertical axis.

In summary, to obtain quasi-independent resonances in the coupling at the interfaces of electromagnetic transverse and longitudinal electromagnetic waves (or plasmons), we applied a hydrodynamic model together with a simple transfer-matrix formalism to the calculation of the electromagnetic reflectance of multilayered systems made of alternated metallic or semiconductor and insulator layers of different thickness. In order to be able to observe many guided-plasmons peaks sufficiently separated in units of the plasma frequency, we chose in our calculations layers of the same materials but different thickness and we found that the width of the layers can be varied to accommodate various peaks in the case of layers made of highly doped semiconductors. In contrast, in the case of systems made of metallic layers described by Drude models, we found that even for very thin layers (of the order of 30 Å) the reflectance peaks are so closely packed together that it would not be possible to accommodate (or resolve easily in units of the plasma frequency) the

peaks resulting of the different families of guided plasmons. In contrast to Ref. 6, where an infinite conductor-insulator superlattice with layers of constant widthwas studied, here we analyze a *finite* superlattice made of only a few layers with different widths (which for many cases it might be a more realistic system), so it can be thought that both works are complementary. On the other hand, we hope that the physical concepts discussed here can help the reader to get a better understanding of the electromagnetic longitudinal-transverse coupling and of the powerful transfer matrix formalism.

Acknowledgments

References

1. For an introduction of the transfer matrix formalism in different branches of physics see, for example, E. Merzbacher, *Quantum Mechanics*, 2nd Edition (Wiley, New York, 1970). Chapter 6; C. Cohen-Tannoudji, B. Diu and F. Laloë, *Quantum Mechanics*, 2nd Edition, Vol I, Complement N_{III} (Wiley, New York, 1977); M. Born and E. Wolf, *Principles of Optics* (MacMillan, New York, 1964). Sec. 1.6; B.L.N. Kennet, *Seismic Wave Propagation in Stratified Media*, (Cambridge University Press, Cambridge, England, 1985), Sec. 2.2.
2. For a modern account of the effects of the longitudinal electromagnetic waves in solids, and nonlocality in general, see the excellent book *Spatial Dispersion in Solids and Plasmas*, edited by P. Halevi (North Holland, Amsterdam, 1992) and references therein.
3. J. Lindhard, *Kgl. Danske Videnskab Selskab, Mat. Fys. Medd.* **28** (1954) 8.
4. I. Lindau and P.O. Nilsson, *Phys. Lett.* **A31** (1970) 352; *Phys. Scr.* **3** (1971) 87.
5. F. Sauter, *Z. Phys.* **203** (1967) 488; F. Fortsmann, *Z. Phys.* **203** (1967) 495; A.R. Melnyk and M.J. Harrison, *Phys. Rev. B* **2** (1970) 835; P.J. Feibelman, *Prog. Surf. Sci.* **12** (1982) 287; P. Apell, *Phys. Scr.* **17** (1978) 535; K. Kempa and W.L. Schaich, *Phys. Rev. B* **34** (1986) 547; R. Kotz, D.M. Kolb, and F. Fortsmann, *Surf. Sci.* **91** (1980) 153; F. Fortsmann and R.R. Gerhardts, *Metal Optics Near the Plasma Frequency*, (Springer, Berlin, 1986) and references therein.
6. W.L. Mochán, M. del Castillo-Mussot, and R.G. Barrera, *Phys. Rev. B* **35** (1987) 1088.
7. D.W. Lynch and W.R. Hunter, "Comments on the Optical Constants of Metals and an Introduction to the data for Several Metals", in: *Handbook of Optical Constant of Solids*, edited by E.D. Palik (Academic, Orlando, 1985).
8. N.W. Ashcroft and N.D. Mermin, *Solid State Physics*, (Holt-Saunder, Philadelphia, 1981).
9. P.J. Feibelman, *Prog. Surf. Sci.* **166** (1982) 287.
10. H.R. Hensen and V. Zauls, *Optics Commun.* **114** (1995) 363.